Electronic Supplementary Information

Synthesis of Bismuth Oxyiodides and Their Composites:

Characterization, Photocatalytic Activity, and Degraded Mechanisms

Wenlian William Lee, [b,c,*] Chung-Shin Lu, [d] Chung-Wei Chuang, [a] Yen-Ju Chen, [a] Jing-Ya Fu, [a] Ciao-Wei Siao, [a] Chiing-Chang Chen [a,*]

[a] Department of Science Application and Dissemination, National Taichung University of Education, Taichung 403, Taiwan, ROC

[b] Department of Occupational Safety and Health, Chung-Shan Medical University, Taichung 402, Taiwan

[c] Department of Occupational Medicine, Chung-Shan Medical University Hospital, Taichung 402, Taiwan

[d] Department of General Education, National Taichung University of Science and Technology, Taichung 404, Taiwan, ROC

* Author to whom correspondence should be addressed

E-mail: ccchen@mail.ntcu.edu.tw; wllee01@gmail.com

Tel: +886-4-2218-3406

Fax: +886-4-2218-3560

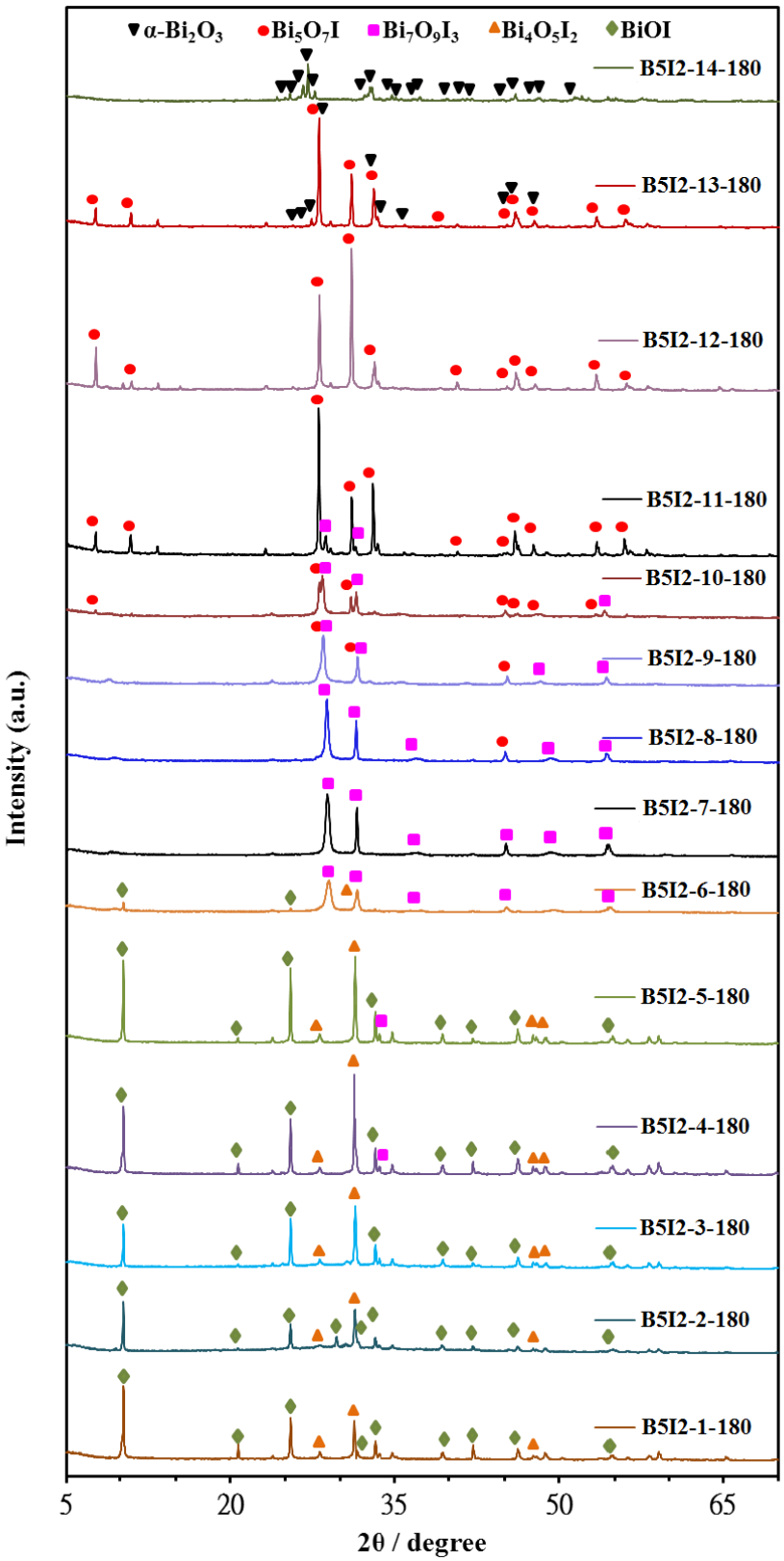

Figure S1. XRD patterns of as-prepared bismuth oxyiodide samples under different pH values, at reaction temperature 180 °C and reaction times 12 h. (Molar ratio $Bi(NO_3)_3$/KI =5/2)

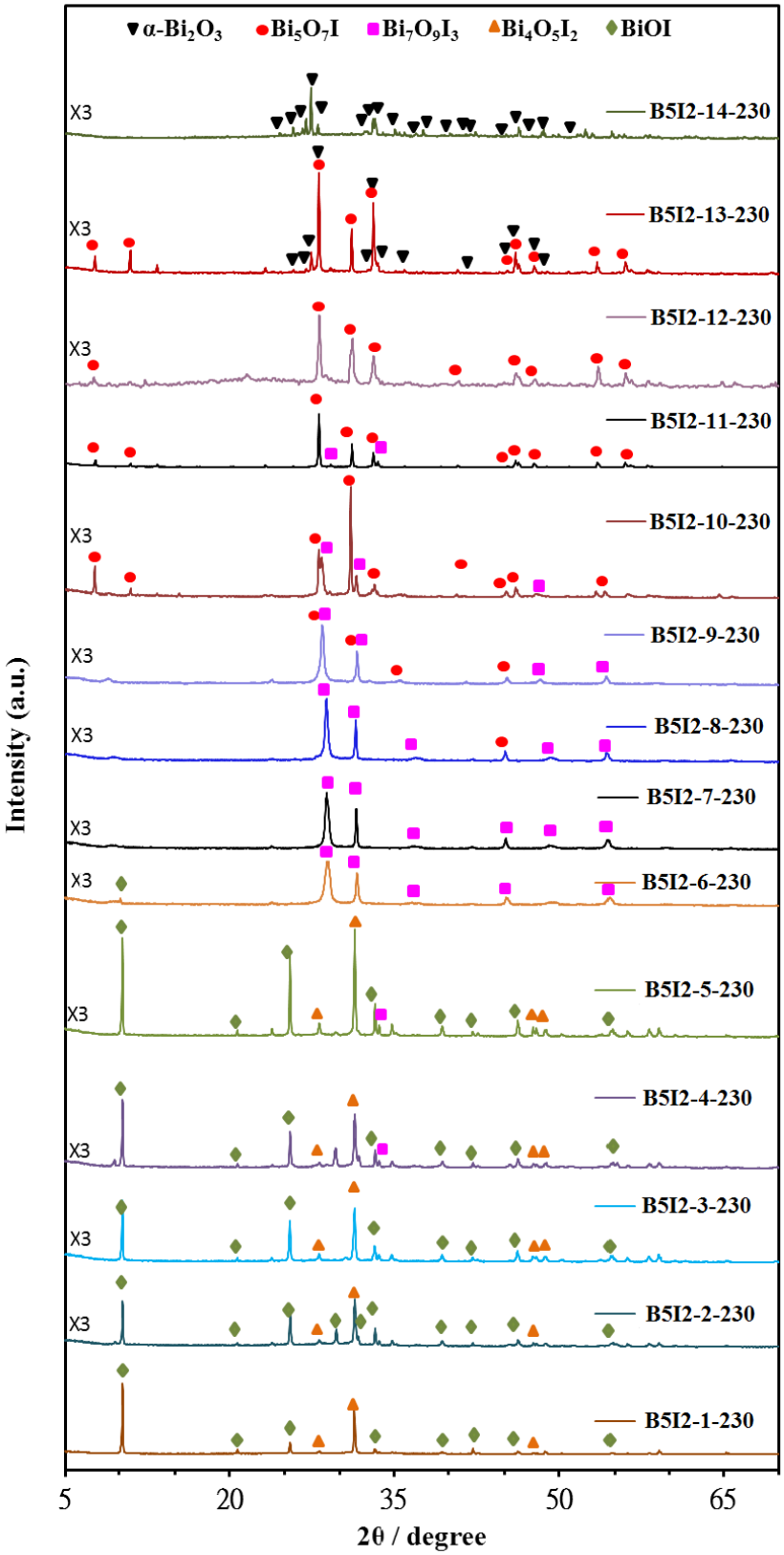

Figure S2. XRD patterns of as-prepared bismuth oxyiodide samples under different pH values, at reaction temperature 230 °C and reaction times 12 h. (Molar ratio $Bi(NO_3)_3$/KI =5/2)

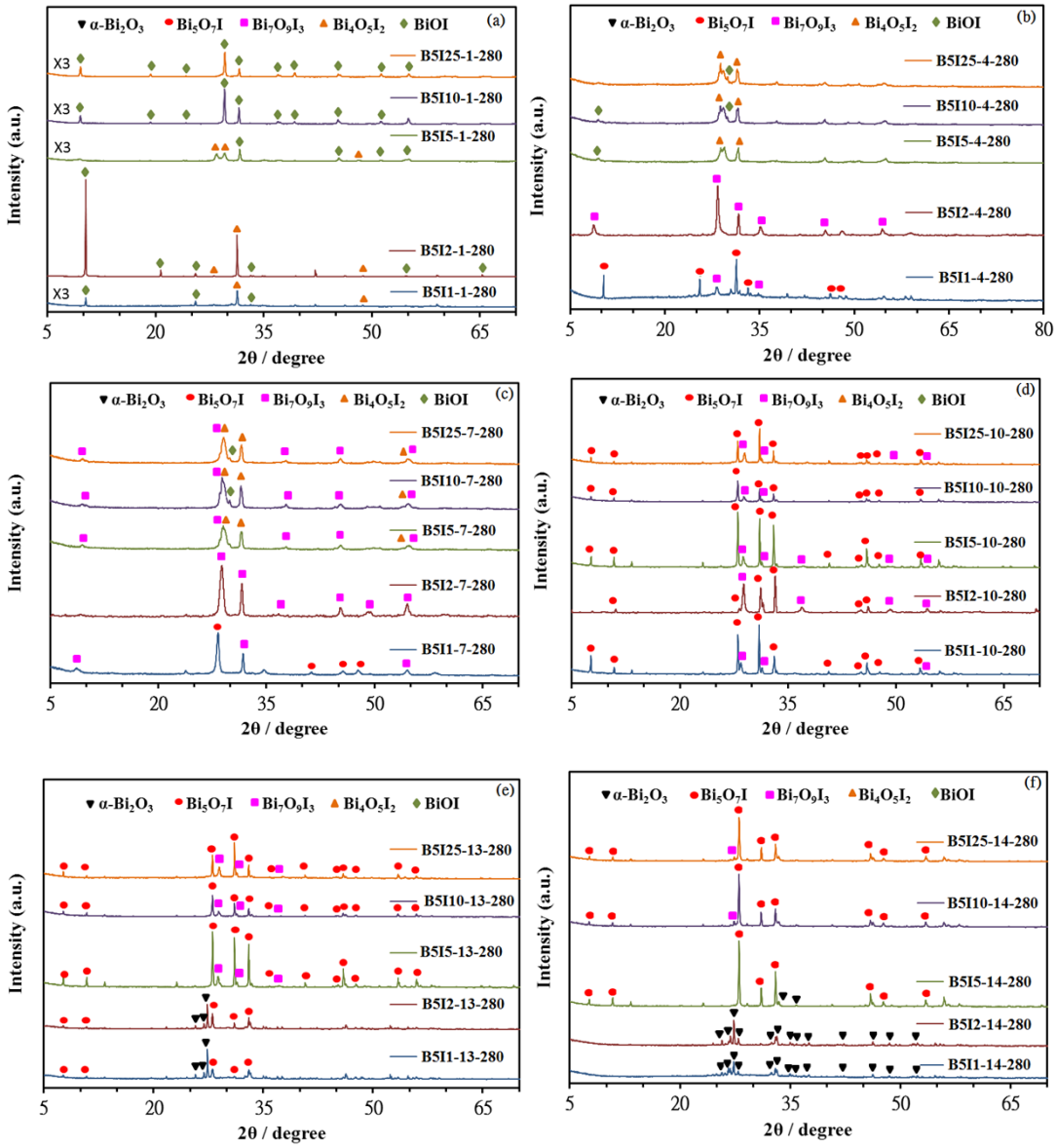

Figure S3. XRD patterns of as-prepared bismuth oxyiodide samples under different molar ratio and at different pH values. (reaction times 12 h and reaction temperature 280 °C)

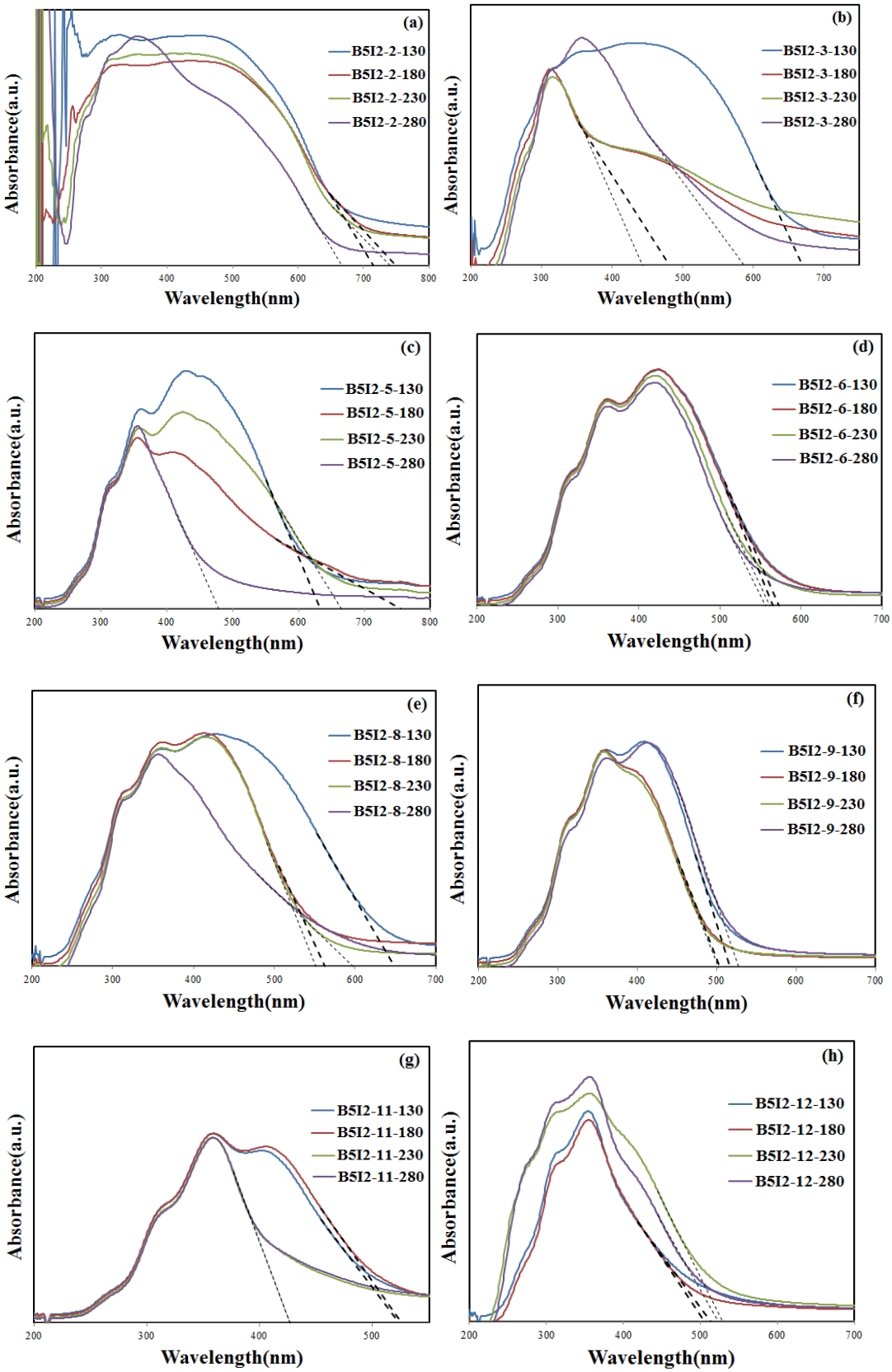
(a)
B5I2-2-130
B5I2-2-180
B5I2-2-230
B5I2-2-280
Absorbance(a.u.)
Wavelength(nm)
(b)
B5I2-3-130
B5I2-3-180
B5I2-3-230
B5I2-3-280
Absorbance(a.u.)
Wavelength(nm)
(c)
B5I2-5-130
B5I2-5-180
B5I2-5-230
B5I2-5-280
Absorbance(a.u.)
Wavelength(nm)
(d)
B5I2-6-130
B5I2-6-180
B5I2-6-230
B5I2-6-280
Absorbance(a.u.)
Wavelength(nm)
(e)
B5I2-8-130
B5I2-8-180
B5I2-8-230
B5I2-8-280
Absorbance(a.u.)
Wavelength(nm)
(f)
B5I2-9-130
B5I2-9-180
B5I2-9-230
B5I2-9-280
Absorbance(a.u.)
Wavelength(nm)
(g)
B5I2-11-130
B5I2-11-180
B5I2-11-230
B5I2-11-280
Absorbance(a.u.)
Wavelength(nm)
(h)
B5I2-12-130
B5I2-12-180
B5I2-12-230
B5I2-12-280
Absorbance(a.u.)
Wavelength(nm)

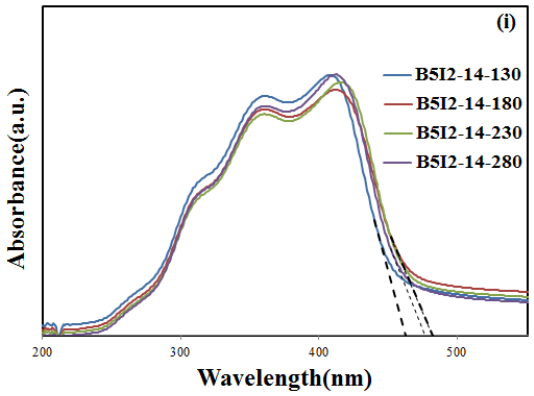

Figure S4. UV-vis absorption spectra of the prepared bismuth oxyiodide catalysts under different pH values and reaction temperature. (Molar ratio $Bi(NO_3)_3$/KI =5/2, reaction time 12h)

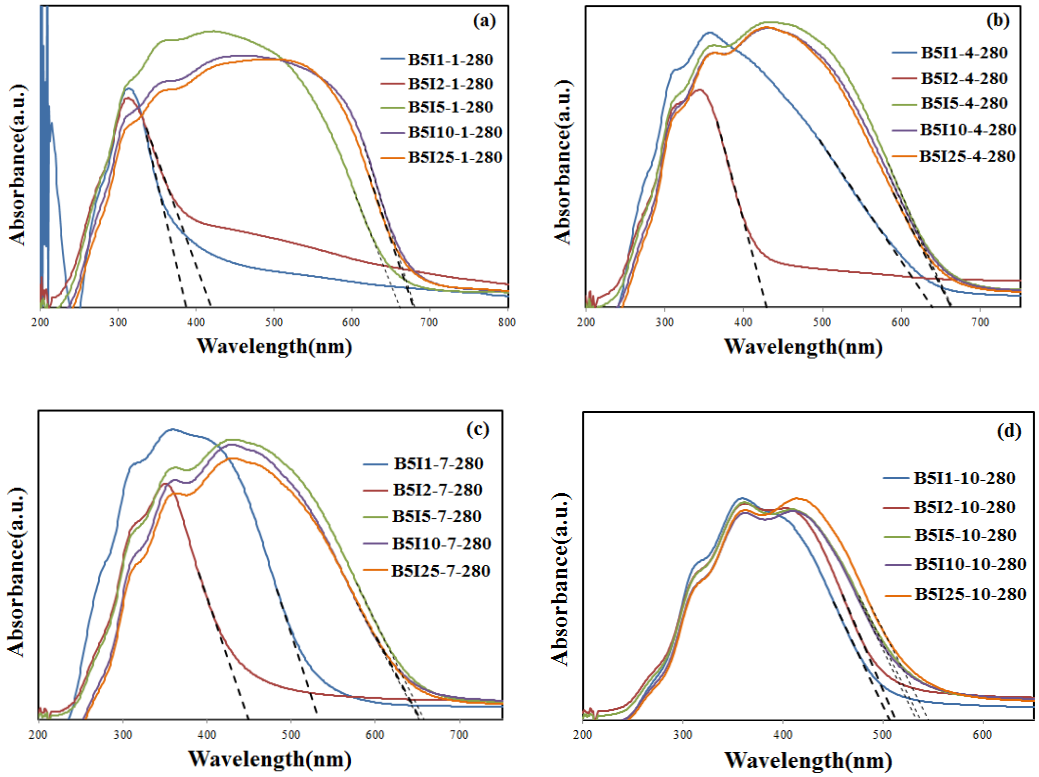

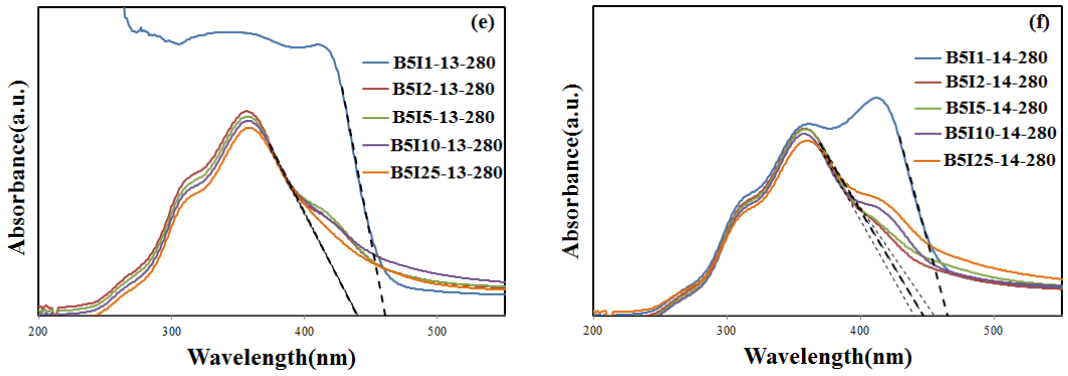

Figure S5. UV-vis absorption spectra of the prepared bismuth oxyiodide catalysts under different pH values. (Hydrothermal conditions: Molar ratio $Bi(NO_3)_3$/KI =5/2, temp = 280 °C, time = 12h)

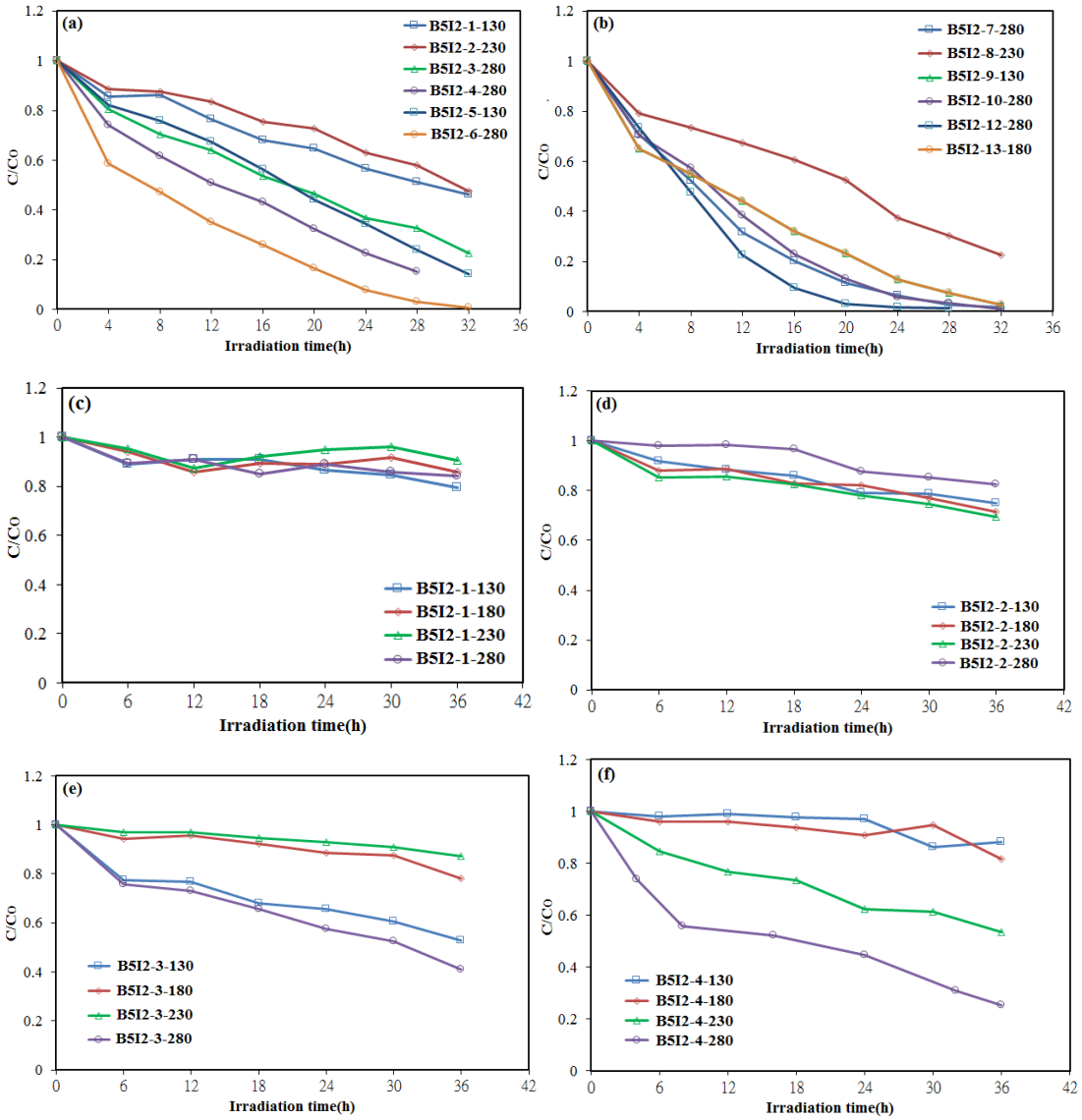

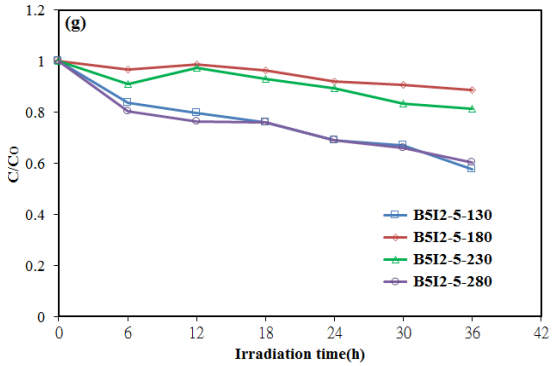
(g)
C/Co
Irradiation time(h)
B5I2-5-130
B5I2-5-180
B5I2-5-230
B5I2-5-280

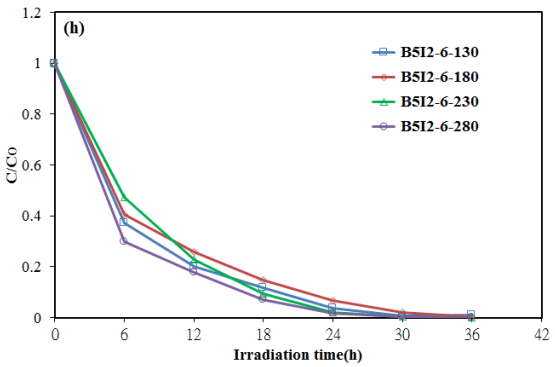
(h)
C/Co
Irradiation time(h)
B5I2-6-130
B5I2-6-180
B5I2-6-230
B5I2-6-280

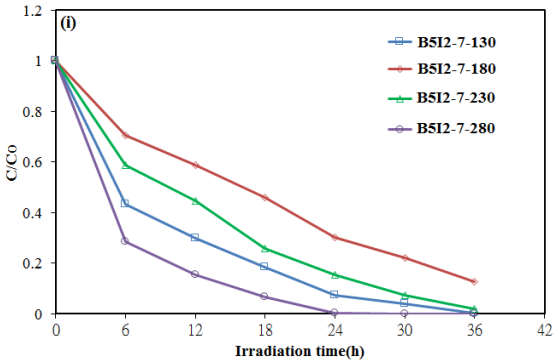
(i)
C/Co
Irradiation time(h)
B5I2-7-130
B5I2-7-180
B5I2-7-230
B5I2-7-280

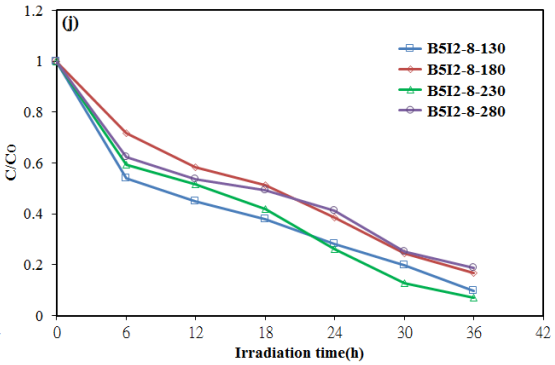
(j)
C/Co
Irradiation time(h)
B5I2-8-130
B5I2-8-180
B5I2-8-230
B5I2-8-280

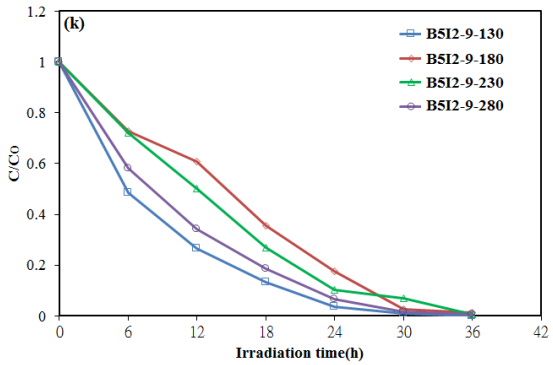
(k)
C/Co
Irradiation time(h)
B5I2-9-130
B5I2-9-180
B5I2-9-230
B5I2-9-280

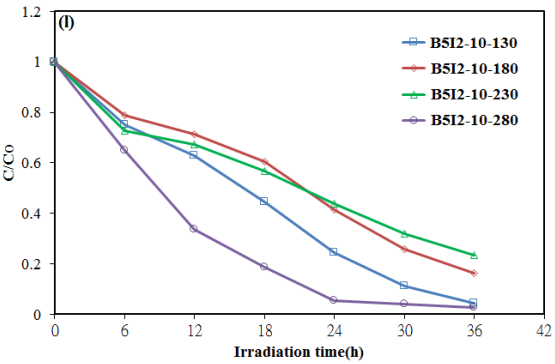
(l)
C/Co
Irradiation time(h)
B5I2-10-130
B5I2-10-180
B5I2-10-230
B5I2-10-280

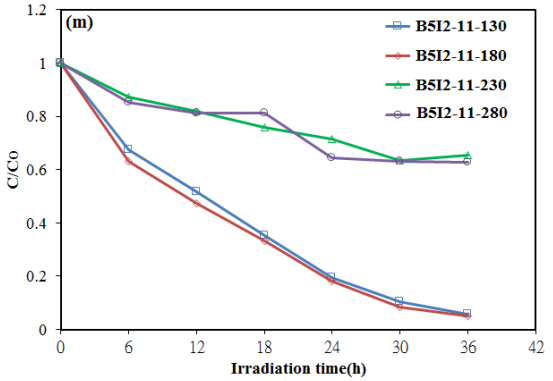
(m)
C/Co
Irradiation time(h)
B5I2-11-130
B5I2-11-180
B5I2-11-230
B5I2-11-280

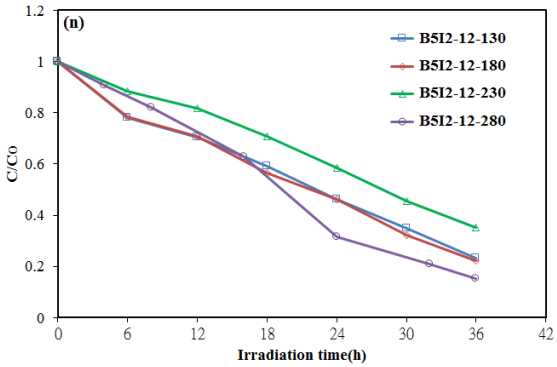
(n)
C/Co
Irradiation time(h)
B5I2-12-130
B5I2-12-180
B5I2-12-230
B5I2-12-280

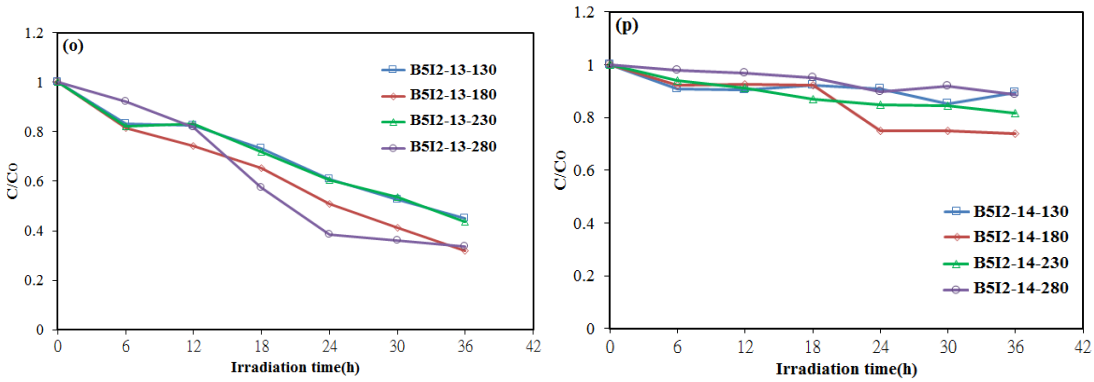

Figure S6. Photodegradation of CV as a function of irradiation time over different Bimuth Oxyiodide photocatalysts. ((Hydrothermal conditions: Molar ratio $Bi(NO_3)_3$/KI =5/2, pH = 1-14, temp = 130-280 ^oC, time = 12h)

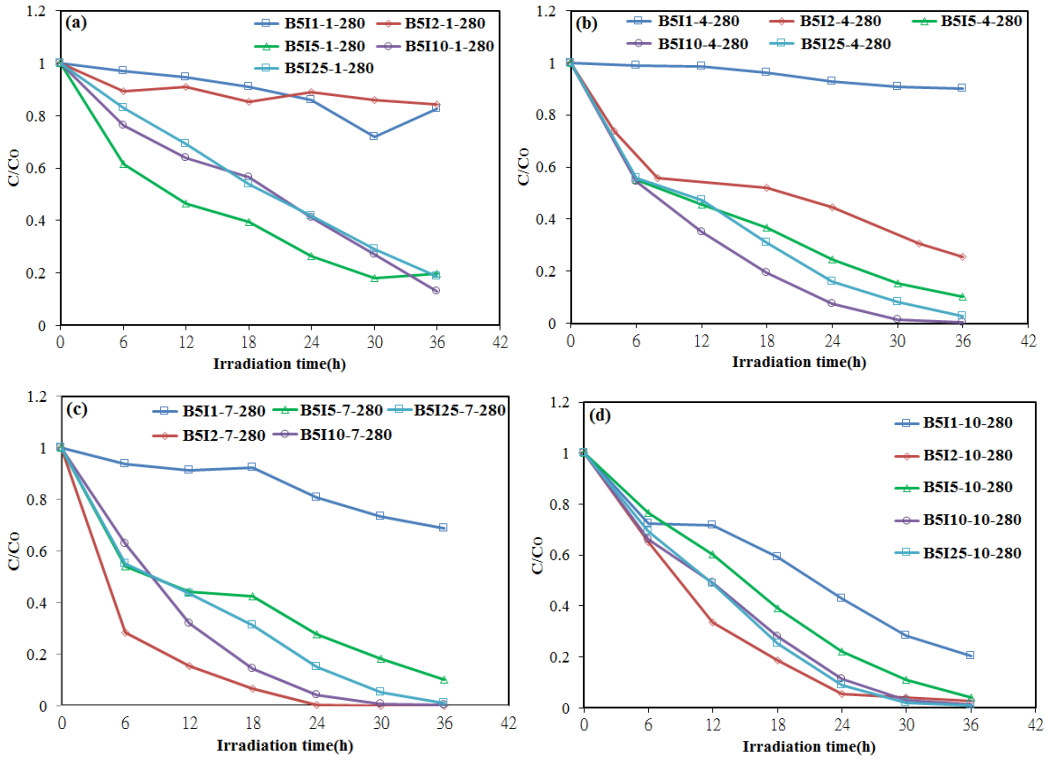

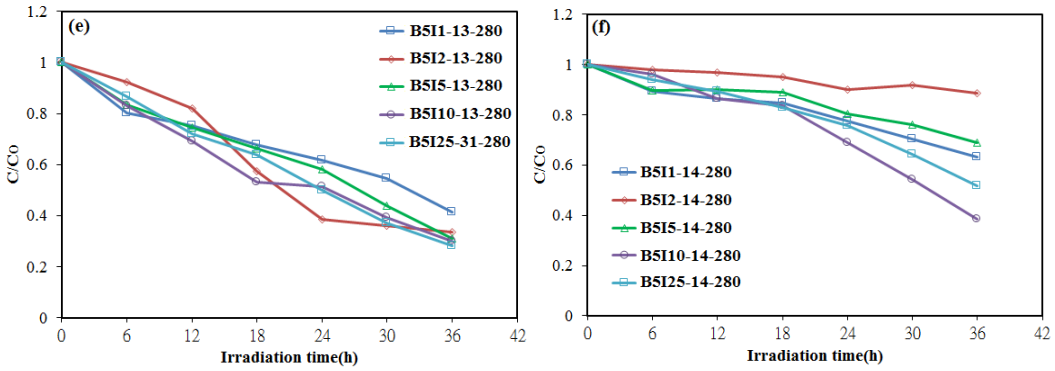

Figure S7. Photodegradation of CV as a function of irradiation time over different Bimuth Oxyiodide photocatalysts. ((Hydrothermal conditions: Molar ratio $Bi(NO_3)_3$/KI =5/2, pH = 1-14, temp = 280 ^oC, time = 12h)

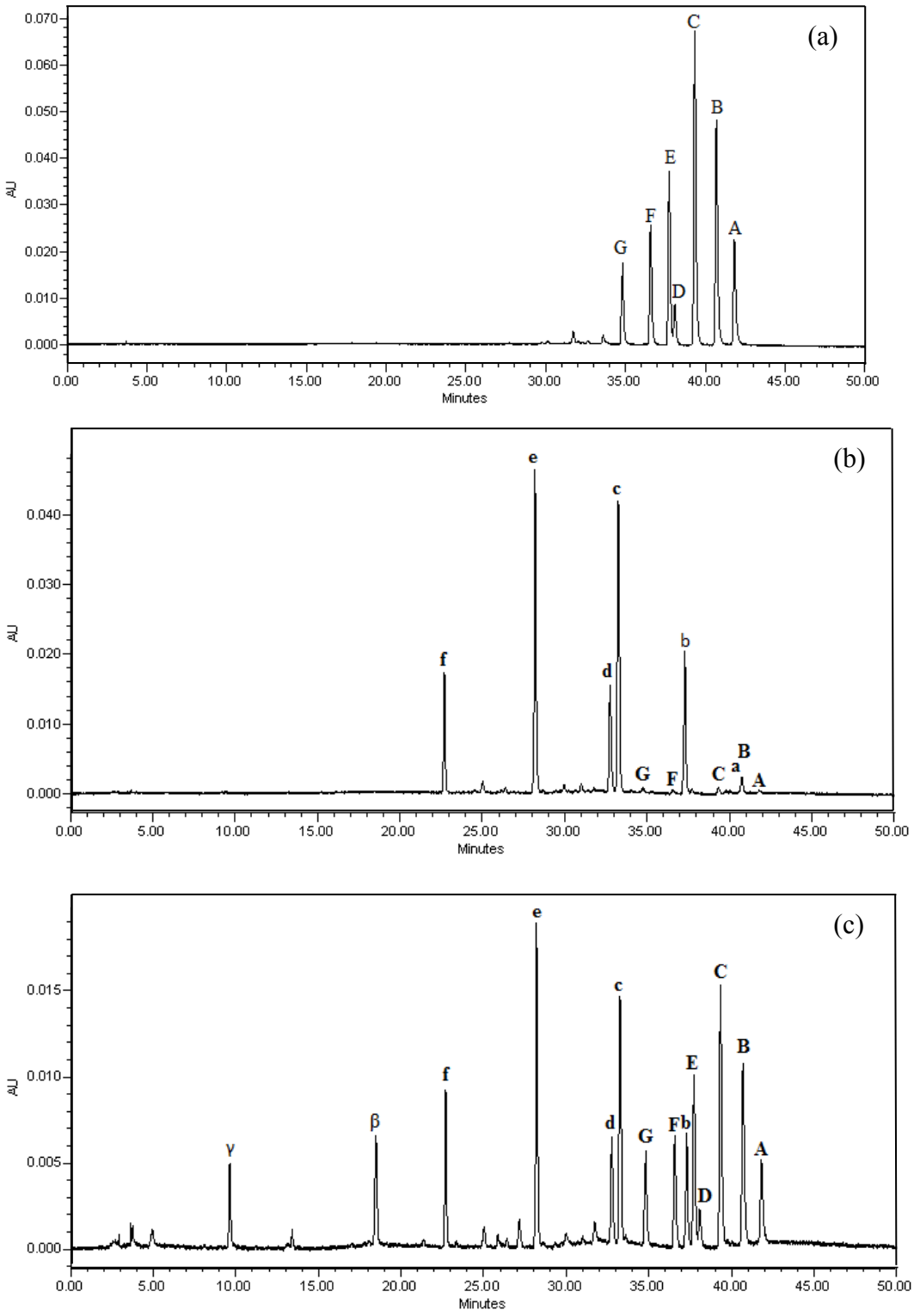

Figure S8. HPLC chromatogram of the degraded intermediates at different irradiation intervals, recorded at (a) 580nm, (b) 350nm, (c) 300nm.

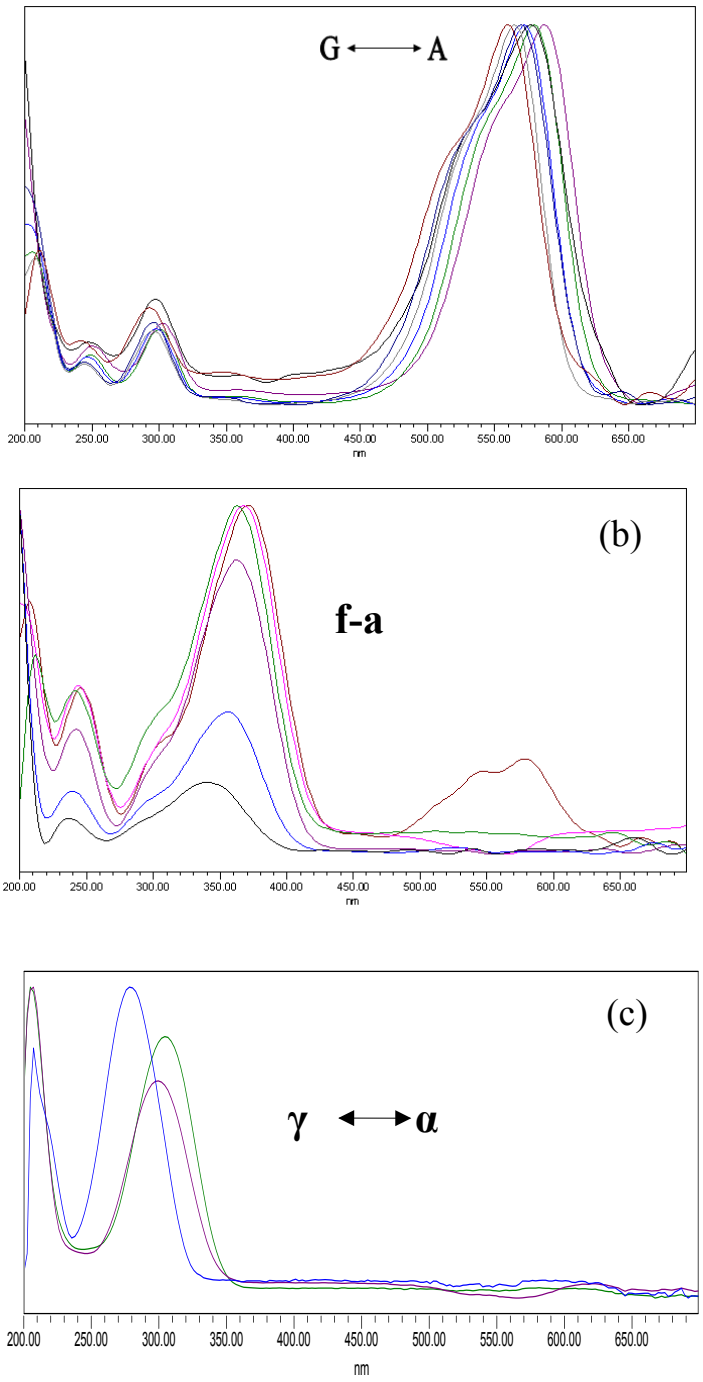

Figure S9. Absorption spectra of the intermediates formed during the photodegradation process of the CV dye corresponding to the peaks in the HPLC chromatograph.

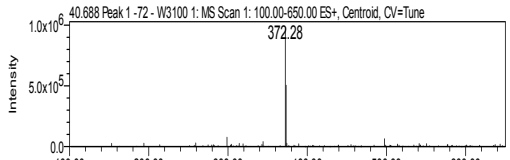

A

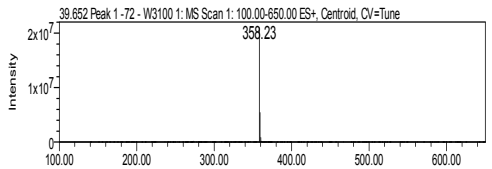

B

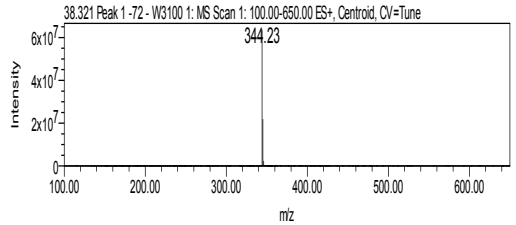

C

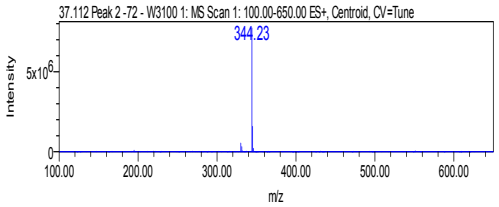

D

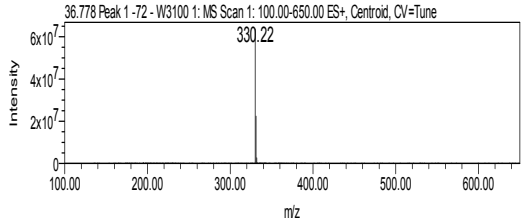

E

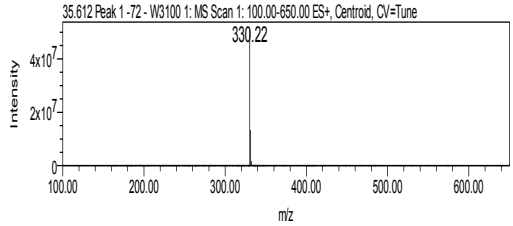

F

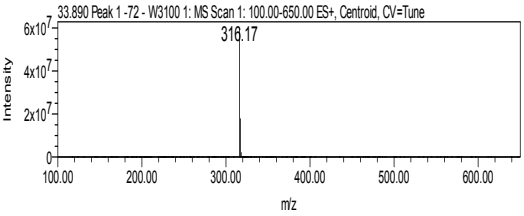

G

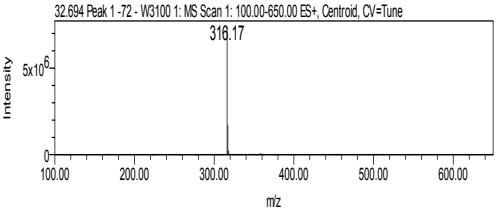

H

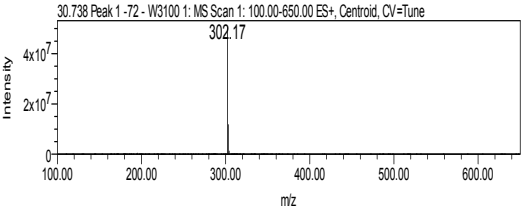

I

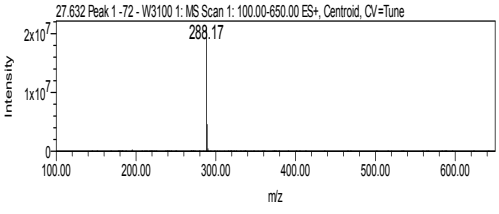

J

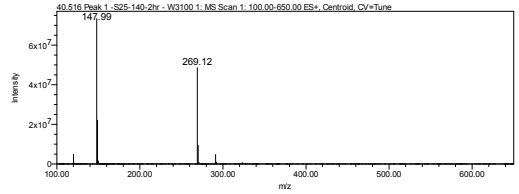

a

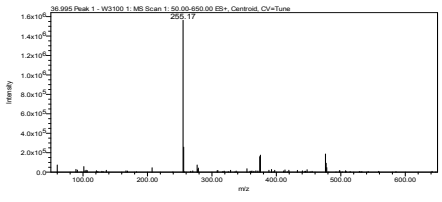

b

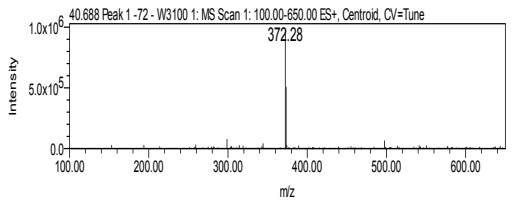

A

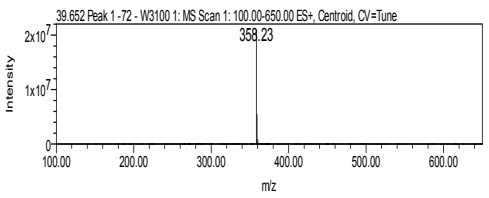

B

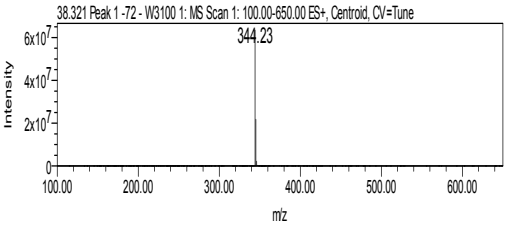

C

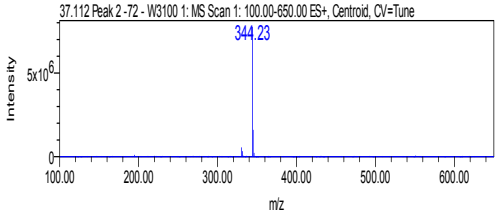

D

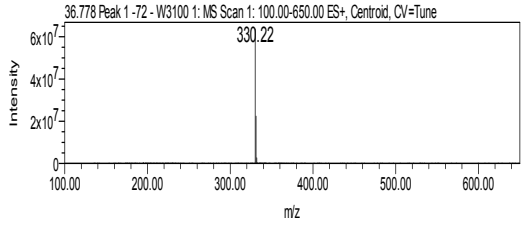

E

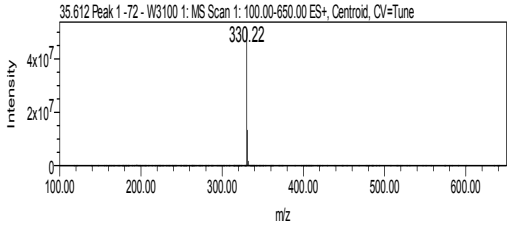

F

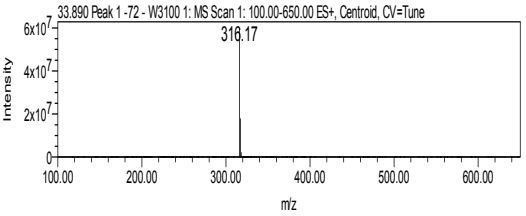

G

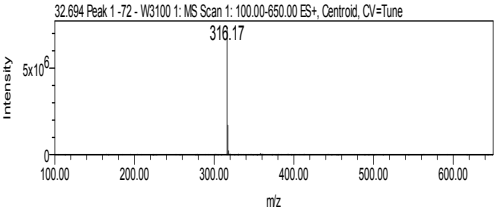

H

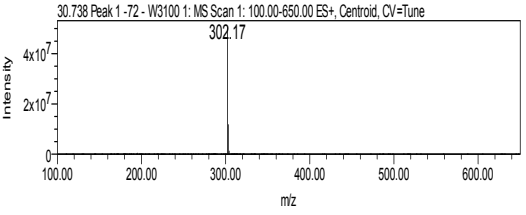

I

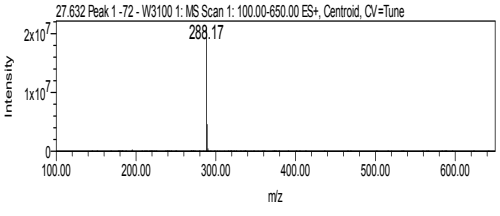

J

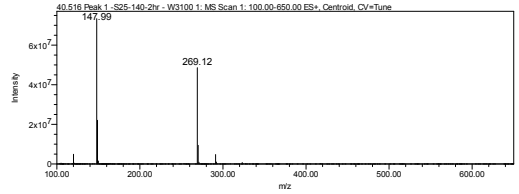

a

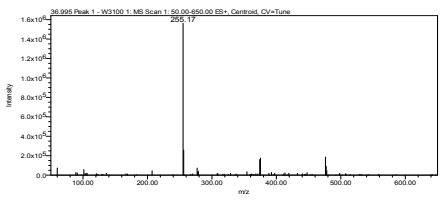

b

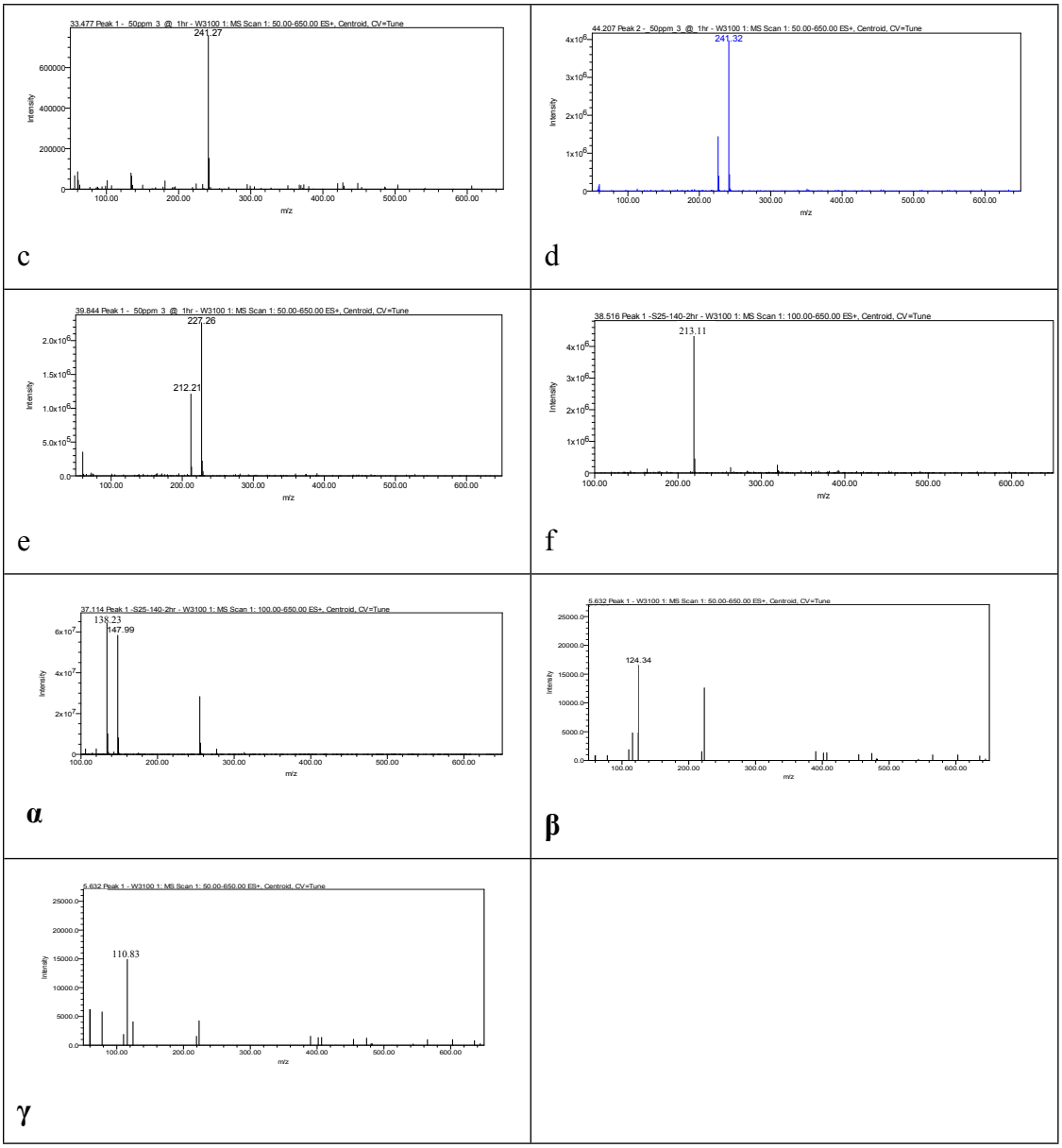

Figure S10. ESI mass spectra of intermediates formed during the photodegradation of the CV dye a fter they were separated by HPLC method.

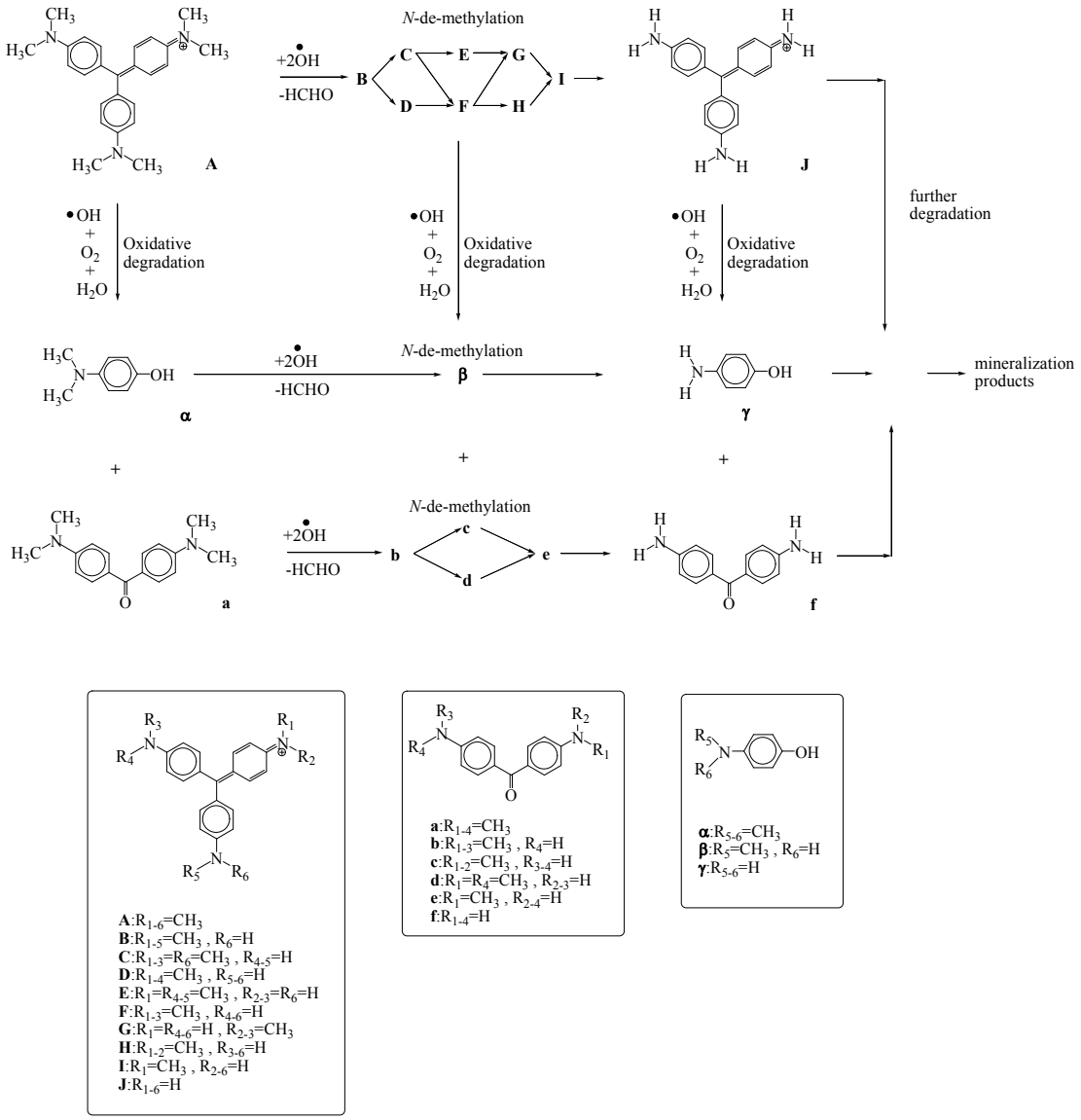

A:$R_{1\text{-}6}$=CH_3
B:$R_{1\text{-}5}$=CH_3 , R_6=H
C:$R_{1\text{-}3}$=R_6=CH_3 , $R_{4\text{-}5}$=H
D:$R_{1\text{-}4}$=CH_3 , $R_{5\text{-}6}$=H
E:R_1=$R_{4\text{-}5}$=CH_3 , $R_{2\text{-}3}$=R_6=H
F:$R_{1\text{-}3}$=CH_3 , $R_{4\text{-}6}$=H
G:R_1=$R_{4\text{-}6}$=H , $R_{2\text{-}3}$=CH_3
H:$R_{1\text{-}2}$=CH_3 , $R_{3\text{-}6}$=H
I:R_1=CH_3 , $R_{2\text{-}6}$=H
J:$R_{1\text{-}6}$=H

a:$R_{1\text{-}4}$=CH_3
b:$R_{1\text{-}3}$=CH_3 , R_4=H
c:$R_{1\text{-}2}$=CH_3 , $R_{3\text{-}4}$=H
d:R_1=R_4=CH_3 , $R_{2\text{-}3}$=H
e:R_1=CH_3 , $R_{2\text{-}4}$=H
f:$R_{1\text{-}4}$=H

α:$R_{5\text{-}6}$=CH_3
β:R_5=CH_3 , R_6=H
γ:$R_{5\text{-}6}$=H

Figure S11. Porposed photodegradation mechanism of the CV dye.

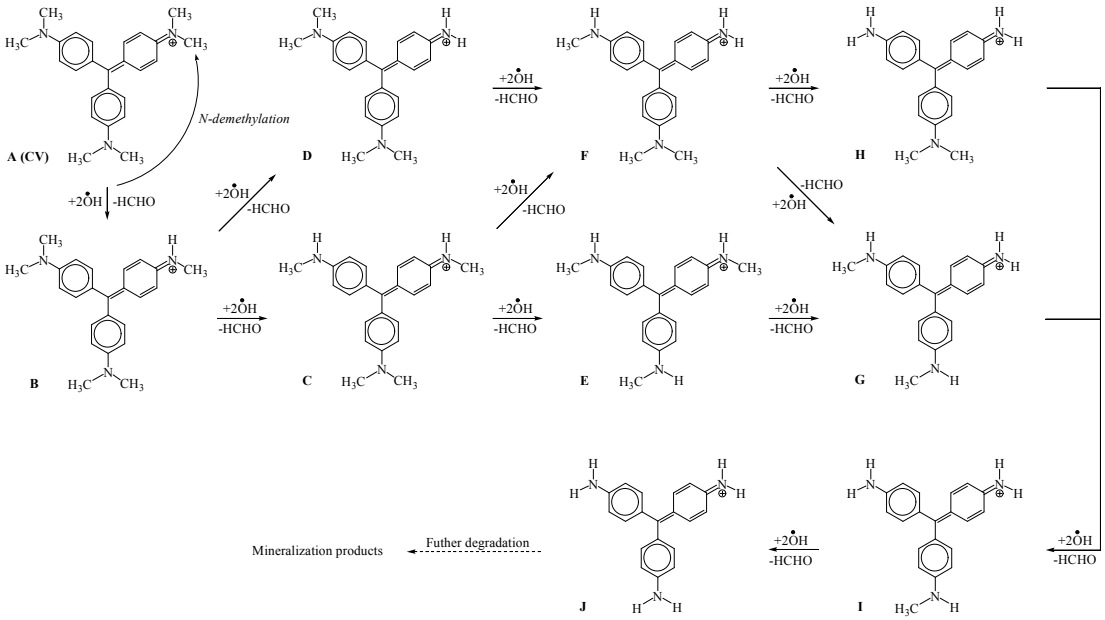

Figure S12. Proposed *N*-de-methylation mechanism of CV with bismuth oxyiodides.

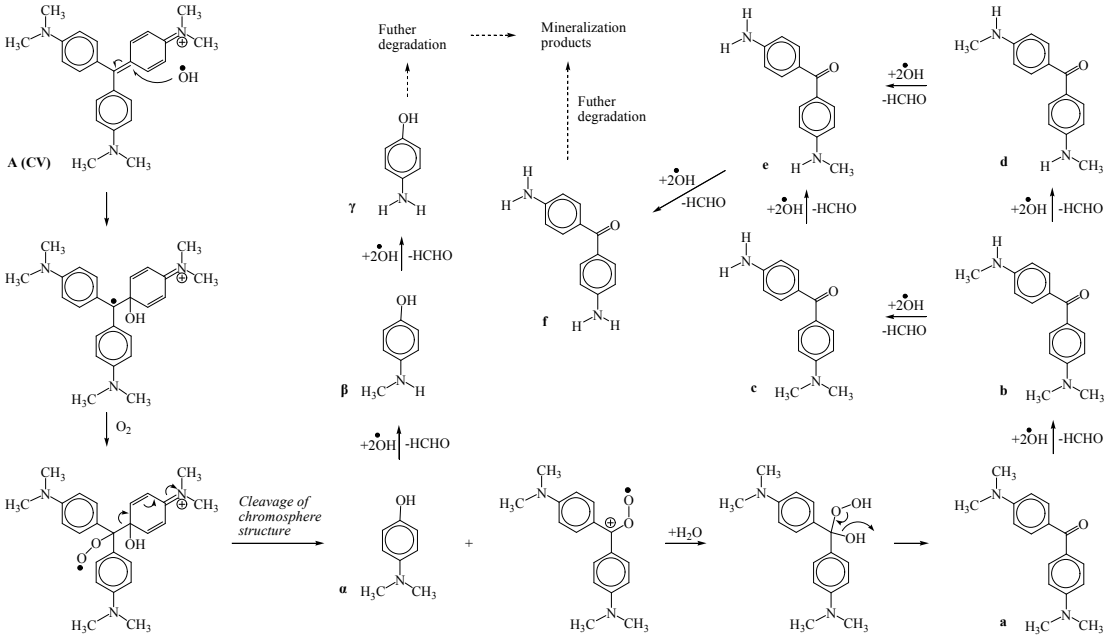

Figure S13. Proposed mechanism of cleavage of chromosphere structure of CV with bismuth oxyiodides.

Table S1. Summary of the CV photocatalytic degradation intermediates identified by the HPLC-PDA-ESI/MS.

HPLC peaks	De-methylation intermediates	ESI/MS molecular ions m/z)	Adsorption maximum (nm)
A	*N*, *N*, *N*′, *N*′, *N*″, *N*″-hexamethyl-pararosaniline	372.28	588.9
B	*N*, *N*-dimethyl-*N*′, *N*′-dimethyl-*N*″-methyl-pararosaniline	358.23	581.1
C	*N*, *N*-dimethyl-*N*′-methyl-*N*″-methyl-pararosaniline	344.23	575.3
D	*N*, *N*-dimethyl-*N*′, *N*′-dimethyl-pararosaniline	344.23	581.6
E	*N*-methyl-*N*′-methyl-*N*″-methyl-pararosaniline	330.22	566.9
F	*N*, *N*-dimethyl-*N*′-methyl-pararosaniline	330.22	570.5
G	*N*-methyl-*N*′-methyl-pararosaniline	316.17	563.8
H	*N*, *N*-dimethyl-pararosaniline	316.17	566.9
I	*N*-methyl-pararosaniline	302.17	555.7
J	pararosaniline	288.17	542.0
a	4-(*N*,*N*-dimethylamino)-4'-(*N*',*N*'-dimethylamino)benzophenone	269.12	377.8
b	4-(*N*, *N*-dimethylamino)-4'-(*N*'-methylamino)benzophenone	255.17	366.9
c	4-(*N*-methylamino)-4'-(*N*'-methylamino)benzophenone	241.27	361.8
d	4-(*N*, *N*-dimethylamino)-4'-aminobenzophenone	241.32	365.4
e	4-(*N*-methylamino)-4'-aminobenzophenone	227.26	358.1
f	4,4'-bis-aminobenzophenone	213.11	340.3
α	4-(*N*, *N*-dimethylamino)phenol	138.23	311.2
β	4-(*N*-methylamino)phenol	124.34	297.7
γ	4-aminophenol	110.23	281.2